

Late spring nitrate distributions beneath the ice-covered Chukchi Shelf

Kevin R. Arrigo¹, Matthew M. Mills¹, Gert L. van Dijken¹, Kate E. Lowry^{1,2}, Robert S. Pickart²,
Reiner Schlitzer³

¹Department of Earth System Science, Stanford University, Stanford, California, USA,

²Department of Physical Oceanography, Woods Hole Oceanographic Institution, Woods Hole, Massachusetts, USA, ³Alfred Wegener Institute, Bremerhaven, Germany

Abstract. Measurements of late springtime nutrient concentrations in Arctic waters are relatively rare due to the extensive sea ice cover that makes sampling difficult. During the SUBICE cruise in May-June 2014, an extensive survey of hydrography and pre-bloom nutrient concentrations was conducted in the Chukchi Sea. Cold ($< -1.5^{\circ}\text{C}$) winter water was prevalent throughout the Chukchi Sea shelf, and the water column was weakly stratified. Nitrate (NO_3^-) concentration averaged $12.6 \pm 1.92 \mu\text{M}$ in surface waters and $14.0 \pm 1.91 \mu\text{M}$ near the bottom and was significantly correlated with salinity. The highest NO_3^- concentrations were associated with winter water within the Central Channel flow path. NO_3^- concentrations were much reduced near the northern shelfbreak within the upper halocline waters of the Canada Basin and along the eastern side of the shelf near the Alaskan coast. Net community production (NCP), estimated as the difference in depth-integrated NO_3^- content between spring (this study) and summer (historical), varied from $28\text{-}38 \text{ g C m}^{-2}$. This is much lower than previous NCP estimates using NO_3^- concentrations from the southeastern Bering Sea as a baseline. These results demonstrate the importance of using local profiles of NO_3^- measured as close to the beginning of the spring bloom as possible when estimating NCP.

1. Introduction

The Chukchi Sea sector of the Arctic Ocean is characterized by its broad and shallow continental shelf, inflow of water from the Bering Sea through Bering Strait [Woodgate *et al.*, 2006], and seasonal but diminishing sea ice cover [Arrigo *et al.*, 2015]. As a result of this loss of sea ice, phytoplankton abundance and rates of net primary production (NPP) have increased dramatically in recent years, both in open water [Arrigo *et al.*, 2015; Belanger *et al.*, 2013] and likely beneath the sea ice [Arrigo *et al.*, 2012; 2014; Zhang *et al.*, 2015].

The high productivity of the Chukchi Sea is maintained by the primarily northward flow of nutrient-rich water through Bering Strait [Woodgate *et al.*, 2006], which spreads over the expansive continental shelf (<200 m depth) and migrates toward the Canada Basin [Zhang *et al.*, 2010; Lowry *et al.*, 2015], although some nutrients are regenerated locally on the shallow shelf [Codispoti *et al.*, 2005]. Circulation on the Chukchi Sea shelf is controlled by bathymetry [Weingartner *et al.*, 2005; Spall, 2007], with three primary flow pathways carrying water northward from the Bering Sea through Bering Strait (Fig. 1). The eastern branch, often referred to in summer as the Alaskan Coastal Current (ACC), is positioned relatively close to the coast and transports warm, fresh, nutrient-poor Alaskan Coastal Water from the Bering Sea and Gulf of Alaska. The central branch flows between Herald Shoal and Hanna Shoal (through Central Channel) and transports both Bering Shelf Water and nutrient-rich Anadyr Water. The western branch contains a large amount of Anadyr Water and flows through Herald Canyon before exiting either to the north off the shelfbreak into the Canada Basin or to the east through Barrow Canyon.

By late spring or summer, the availability of nutrients in the northern Chukchi Sea, particularly dissolved inorganic nitrogen (DIN) such as nitrate (NO_3^-) and ammonium (NH_4^+), is restricted to subsurface reservoirs of winter water (WW), which eventually limits phytoplankton growth [Codispoti *et al.*, 2009; Lowry *et al.*, 2015]. This important summer nutrient resource is associated with the slower interior shelf pathways where WW has not yet flushed off the Chukchi Shelf into the Canada Basin [Lowry *et al.*, 2015, Pickart *et al.*, 2016]. Further south within the Chukchi Sea, open water blooms can remain prominent in spring and summer

wherever nutrient-rich summertime Anadyr Water continues to enter through Bering Strait [Wang *et al.*, 2005].

As phytoplankton deplete surface waters of nutrients, their growth rates at the depth of the nutricline eventually exceed those in near-surface waters, despite lower light levels. High UVR fluxes can also reduce algal growth in near-surface waters [Hessen *et al.*, 2012]. The result is that, over the growth season, phytoplankton populations move deeper in the water column as light increases and the nutricline is progressively depressed, often forming a distinct subsurface chlorophyll maximum (SCM) at depths of 20-40 m [Martin *et al.*, 2010; Brown *et al.*, 2015a]. Measurements of this progressive depletion of nutrients in surface waters have been used to estimate net community production (NCP), a quantity approximately equivalent to new production when the nutrient of interest is NO_3^- [Eppley and Peterson, 1979].

However, obtaining accurate estimates of NCP has been hampered by our poor understanding of pre-bloom NO_3^- distributions on the Chukchi Shelf. The vast majority of nutrient data for this region has been collected during the summer and fall months when nutrient concentrations in surface waters are already reduced to growth-limiting levels [Codispoti *et al.*, 2013]. The handful of nutrient samples obtained in the spring when substantial amounts of sea ice are still present suggest that the Chukchi Shelf is relatively well mixed prior to the initiation of the spring bloom, but the spatial coverage of these samples is extremely limited [Codispoti *et al.*, 2005].

Here we present hydrographic data collected during the Study of Under-ice Blooms In the Chukchi Ecosystem (SUBICE) program in May-June 2014. This is the most spatially extensive dataset on pre-bloom nutrient distributions in the ice-covered northern half of the Chukchi Sea collected to date that can be used 1) to better understand nutrient cycling on the Chukchi Shelf, 2) to track the flow of different water masses from the Bering Sea, over the Chukchi Sea shelf, and into the Beaufort Sea and Canada Basin, and 3) as a baseline from which to more accurately estimate net community production (NCP).

2. Methods

The SUBICE field campaign was conducted in the Chukchi Sea aboard USCGC *Healy* from 13 May – 23 June 2014. During the field expedition, the SUBICE team sampled the water column at 230 hydrographic stations, primarily on the continental shelf of the northeastern Chukchi Sea (Fig. 1). Here we focus on 117 pre-bloom stations that were sampled within the ice pack during the early part of the cruise. At each station, conductivity-temperature-depth (CTD) casts were made using dual temperature (SBE3), conductivity (SBE4c), and pressure (Digiquartz 0-10,000 psi) sensors attached to the ship's 30-liter, 12-position Niskin bottle rosette system. The CTD sensors underwent laboratory calibrations before and after the cruise, with calculated uncertainties of 0.001°C for temperature and 0.008 for salinity. Additional sensors on the rosette included dissolved oxygen (SBE43), photosynthetically active radiation (PAR) (Biospherical QSP-2300), and fluorescence (WET Labs ECO-AFL/FL).

Currents were measured using the ship's hull-mounted Ocean Surveyor 150 KHz unit (OS150) Acoustic Doppler Current Profiler (ADCP) system. Because of the heavy ice, the data were not usable while the ship was steaming, hence profiles were only obtained at the station sites. The data were processed following the procedure outlined in *Pickart et al.* [2016], which includes removing the barotropic tidal signal using the Oregon State University tidal model <http://volkov.oce.orst.edu/tides> [*Padman and Erofeeva, 2004*]. The uncertainty in velocity is <2 cm s⁻¹.

Discrete seawater samples were collected at a set of standard depths (2, 5, 10, 25, 50, 75, and 100 m) in addition to the depth of the subsurface fluorescence maximum (if present) and near the bottom (typically 2-3 m above the seafloor). Nutrient analysis was performed onboard the ship using a Seal Analytical continuous flow Auto-Analyzer 3 and a modification of the method in *Armstrong et al.* [1967] to measure the concentrations of nitrate (NO₃⁻), ammonium (NH₄⁺), nitrite (NO₂⁻), phosphate (PO₄³⁻), and silicate (Si(OH)₄). Seawater samples for dissolved oxygen (O₂) were analyzed using standard Winkler titrations to calibrate sensor measurements from the CTD casts. For analysis of chlorophyll *a* (Chl *a*) concentration, seawater was filtered onto 25

mm Whatman GF/F filters (0.7 μm nominal pore size). Filters were extracted in the dark in 5 mL of 90% acetone for 24 hrs at +3°C prior to measurement [Holm-Hansen *et al.*, 1965] on a Turner Designs 10-AU fluorometer calibrated with pure Chl *a* (Sigma-Aldrich). Particulate organic carbon and nitrogen (POC and PON) samples were filtered through 25 mm GF/Fs. Blank filters were made daily by filtering ~25 ml filtered (0.2 μm) seawater through filters and processing the same as the particulate samples. Filters were immediately dried at 60°C and stored dry until processing. Prior to analysis, samples were fumed with concentrated HCl, dried in a low temperature oven at 60°C, and packed into tin capsules (Costech Analytical Technologies, Inc.) for analysis. Samples were analyzed on an Elementar Vario EL Cube or Micro Cube elemental analyzer (Elementar Analysensysteme GmbH, Hanau, Germany) which was interfaced to a PDZ Europa 20-20 isotope ratio mass spectrometer (Sercon Ltd., Cheshire, UK). Calibration standards were glutamic acid and peach leaves.

NCP was calculated by using our pre-bloom NO_3^- concentration profiles on the Chukchi shelf as a baseline and using data from historical summer cruises to the region to determine the depth of NO_3^- depletion, assuming that NO_3^- concentrations above that depth were reduced to zero. The vertical integral of this NO_3^- depletion was then assumed to be equal to NCP, which was converted to carbon (C) units assuming a molar C:N uptake ratio of 6.0 [Hansell *et al.*, 1993].

3. Pre-bloom hydrography

Most of the SUBICE study was conducted in shallow (40-50 m) continental shelf waters that were covered by 1.0-1.5 m of sea ice and 0.02-0.15 m of snow. Sea ice concentrations at the 117 stations focused on here were approximately 100%, as determined by two-hourly ship observations and passive microwave satellite data (Fig. 1). The surface melt ponds that are common in summer [Arrigo *et al.*, 2014] were absent during our study due to persistently sub-freezing air temperatures.

Over much of the northeast Chukchi shelf, seawater temperature and salinity fell within a narrow range of -1.55°C to -1.78°C and 32 to 33, respectively (Fig. 2), demonstrating that in the late spring, the shelf is comprised almost exclusively of WW [Carmack, 2000]. At the northernmost stations sampled near the shelfbreak, waters were similarly cold, but much fresher (salinity of 30.5 to 32) than on the shelf, indicating the presence of early-season meltwater. Remnant winter water (RWW) was also found seaward of the shelfbreak. This water mass is one of the main constituents of the cold halocline of the Canada Basin [Anderson et al., 2013]. In the southern part of the domain, beneath the pack ice, the water was close to the freezing point over a range of salinities. This is referred to as newly ventilated winter water (NVWW), having been formed during the preceding winter. Temperature (Fig. 3a) and salinity (Fig. 3b) sections indicate that shelf waters were two-layered but weakly stratified, and that the strength of the horizontal gradients in salinity and temperature exceeded that of the vertical gradients in most areas.

Oxygen saturation (80-85%) and concentrations of Chl *a* ($<1\text{ mg m}^{-3}$), POC ($<60\text{ mg m}^{-3}$), and PON ($<70\text{ mg m}^{-3}$) were generally low on the shelf, indicating that the phytoplankton bloom had not yet begun in waters beneath the sea ice during the early part of the cruise. Nitrate (NO_3^-) concentrations under the ice were high virtually everywhere on the shelf and highly correlated with salinity (Fig. 4), except for the far eastern and northern regions of our study area where nutrient concentrations were very low in the basin and near the coast (Fig. 3c). Over much of the shelf, the two-layered water column had surface and near bottom NO_3^- concentrations that averaged $12.6 \pm 1.92\ \mu\text{M}$ and $14.0 \pm 1.91\ \mu\text{M}$, respectively.

Although NO_3^- concentrations were high almost everywhere on the shelf, those along the main flow paths across the Chukchi Sea shelf (e.g., the Central Channel jet) were generally 3-5 μM higher than concentrations in the surrounding areas (Fig. 3c). Based on the ADCP data, we identified the presence of the main flow pathways. Consistent with previous studies (Weingartner et al., 2013; Pickart et al., 2016), we found that the Central Channel pathway is augmented by flow from the west (likely from Herald Canyon), and, upon encountering Hanna

Shoal, the pathway bifurcates (Fig. 3c). Maximum velocities within these jets ($0.20\text{-}0.25\text{ m s}^{-1}$) are much higher than velocities over the rest of the shelf and carry a higher fraction of high NO_3^- from the Bering Sea, as indicated by their relatively high salinity (Fig. 3b)(salinity = 32.5-33.0, *Coachman et al.*, 1975). However, in the waters adjacent to the jets, NO_3^- concentrations were also generally in excess of $10\text{ }\mu\text{M}$. Convective overturning was likely taking place during the first part of our survey within small leads in the pack ice. Due to the weak stratification, the overturning would readily reach the bottom and stir regenerated nutrients from the seafloor into the water column. Hence the high NO_3^- concentrations in these waters indicate that local sources augment the nutrients that are transported through Bering Strait.

4. Estimates of NCP

Surface water concentrations of NO_3^- , PO_4^{3-} , and Si(OH)_4 on the Chukchi Shelf measured during SUBICE were much higher than those measured later in the season in the same region, due to assimilation by phytoplankton during spring and summer [*Hansell et al.*, 1993; *Arrigo et al.*, 2014; *Lowry et al.*, 2015]. Therefore, the horizontal distribution of pre-bloom NO_3^- concentrations can be used with nitricline depth measured later in the season to determine minimum estimates of NCP on the Chukchi Sea shelf. Summer cruises to the Chukchi Sea have shown that NO_3^- is fully depleted by phytoplankton down to an average depth of 30 m by mid-July, often in areas where sea ice concentration was still near 100% [*Varela et al.*, 2013; *Arrigo et al.*, 2012; 2014; *Brown et al.*, 2015a; *Lowry et al.*, 2015]. Given the pre-bloom NO_3^- concentrations we measured in the upper 30 m, this yields a mean NCP estimate of $27.8\pm 4.13\text{ g C m}^{-2}$.

Because phytoplankton growth and nutrient consumption continues to erode the nitricline after mid July [*Codispoti et al.*, 2005; *Brown et al.*, 2015a], we also computed NCP from our pre-bloom NO_3^- data using two other assumptions, 1) that NO_3^- was completely consumed within the upper 40 m of the water column, and 2) that NO_3^- was completely consumed throughout the entire water column (this represents an unlikely, but maximum possible, estimate for NCP). As

the nitricline deepens to 40 m, time- and depth-integrated NCP increases to $37.6 \pm 5.59 \text{ g C m}^{-2}$, approximately 35% higher than the mean NCP for a 30 m nitricline. If pre-bloom NO_3^- is fully consumed throughout the water column on the shallow (<50 m) shelf, NCP only increases by another 12.5%, to $42.3 \pm 6.89 \text{ g C m}^{-2}$. These estimates of NCP do not include the low values measured in the northern Chukchi Sea near the shelfbreak ($5\text{-}20 \text{ g C m}^{-2}$) that are associated with the persistently low NO_3^- waters of the Canada Basin [Codispoti *et al.*, 2013].

Our values are on the low end of previous estimates of NCP for the southern ($40\text{-}70 \text{ g C m}^{-2}$) and western (70 g C m^{-2}) Chukchi Sea [Hansell *et al.*, 1993; Codispoti *et al.*, 2013; Mills *et al.*, 2015] using the same approach. The primary reason for this NCP difference is the higher pre-bloom NO_3^- concentrations used in previous studies that were based on a small amount of data in the Chukchi Sea or measurements from upstream in the Bering Sea. For example, Hansell *et al.* [1993] estimated NCP using pre-bloom NO_3^- values that were based on a regression between NO_3^- concentration and salinity for the southeastern Bering Sea. This regression yielded a NO_3^- concentration of $23.2 \text{ }\mu\text{M}$ at a salinity of 33, much higher than the pre-bloom value of $<18 \text{ }\mu\text{M}$ NO_3^- we measured at that same salinity on the Chukchi Sea shelf (Fig. 4). These higher initial NO_3^- concentrations in Hansell *et al.* [1993] would yield larger NO_3^- deficits and greater estimates of NCP in the southern and western Chukchi Sea.

This $5 \text{ }\mu\text{M}$ difference in pre-bloom NO_3^- concentration at a salinity of 33 between water in the southeastern Bering Sea and that on the Chukchi Sea shelf is likely due an imbalance between the processes that alter NO_3^- concentrations during transit between the two regions and need to be accounted for when estimating NCP. For example, the microbial conversion of NO_3^- to N_2 via sediment denitrification has been shown to result in a significant loss of fixed N on both the Bering and Chukchi Sea shelves [Chang and Devol, 2009; Devol *et al.*, 1997; Granger *et al.*, 2011; Haines *et al.*, 1981; Koike and Hattori, 1979; Mills *et al.*, 2015; Tanaka *et al.*, 2004]. Furthermore, the sediments of the Bering and Chukchi Sea are sites of active coupled partial nitrification-denitrification (CPND) [Granger *et al.*, 2011] while the deeper portions of the water column are sites of nitrification [Brown *et al.*, 2015b; Hartnett, 1998; Henriksen *et al.*,

1993], resulting in the regeneration of NO_3^- from ammonified organic N. The net $5 \mu\text{M}$ decrease in NO_3^- between the Bering and Chukchi seas indicates that losses of NO_3^- through denitrification outweigh the gains from nitrification. Because both processes are active throughout the year, estimates of initial NO_3^- concentrations used in NCP calculations for a given region should be based on local profiles of NO_3^- measured as close to the beginning of the spring bloom as possible.

Estimating local NCP from NO_3^- deficits is further complicated in the Chukchi Sea by the fact that waters continue to advect through the Bering Strait and spread out over the Chukchi Sea shelf before entering the Canada Basin and western Beaufort Sea after the spring bloom has begun. In late spring and summer, these northward flowing waters can harbor NO_3^- deficit signatures that originate in phytoplankton blooms within ice-free waters to the south, either in the northern Bering or the southern Chukchi Sea (Fig. 1). The same is true for NO_3^- -depleted waters from the Canada Basin that are transported onto the Chukchi shelf. During our SUBICE cruise, we first observed NO_3^- -depleted waters beneath fully consolidated sea ice and snow in the narrow but rapidly-flowing mid-shelf jet that had penetrated into the sea ice zone, reaching as far north as 71.4°N by June 18. While adjacent areas of the shelf were much less impacted, advection of this reduced- NO_3^- water will markedly alter estimates of local NCP if not properly considered. Accounting for advection of different water masses is particularly important when estimating the relative proportion of NCP taking place beneath the sea ice and in ice-free waters on the Chukchi Sea shelf where ice cover has been changing dramatically in recent decades [Arrigo and Van Dijken, 2015].

Acknowledgements. We thank the captain and crew of the USCGC *Healy* and the SUBICE scientific team. This research was sponsored by the NSF Office of Polar Programs (PLR-1304563 to KRA).

References

- Anderson, L. G., P. S. Andersson, G. Björk, E. Peter Jones, S. Jutterström, and I. Wåhlström (2013), Source and formation of the upper halocline of the Arctic Ocean, *J. Geophys. Res. Oceans*, *118*, 410–421, doi:10.1029/2012JC008291.
- Armstrong, F., C. R. Stearns, and J. Strickland (1967), The measurement of upwelling and subsequent biological process by means of the Technicon Autoanalyzer® and associated equipment, *Deep-Sea Res.*, *14*, 381–389, doi:10.1016/0011-7471(67)90082-4.
- Arrigo, K. R., D. K. Perovich, R. S. Pickart, Z. W. Brown, G. L. van Dijken, K. E. Lowry, M. M. Mills, M. A. Palmer, W. M. Balch, F. Bahr, N. R. Bates, C. Benitez-Nelson, B. Bowler, E. Brownlee, J. K. Ehn, K. E. Frey, R. Garley, S. R. Laney, L. Lubelczyk, J. Mathis, A. Matsuoka, B. G. Mitchell, G. W. K. Moore, E. Ortega-Retuerta, S. Pal, C. M. Polashenski, R. A. Reynolds, B. Scheiber, H. M. Sosik, M. Stephens, and J. H. Swift (2012), Massive phytoplankton blooms under Arctic sea ice, *Science*, *336*, 1408.
- Arrigo, K. R., D. K. Perovich, R. S. Pickart, Z. W. Brown, G. L. van Dijken, K. E. Lowry, M. M. Mills, M. A. Palmer, W. M. Balch, N. R. Bates, C. R. Benitez-Nelson, E. Brownlee, K. E. Frey, S. R. Laney, J. Mathis, A. Matsuoka, B. G. Mitchell, G. W. K. Moore, R. A. Reynolds, H. M. Sosik, and J. H. Swift (2014), Phytoplankton blooms beneath the sea ice in the Chukchi Sea, *Deep-Sea Res., Part II*, *105*, 1-16, <http://dx.doi.org/10.1016/j.dsr2.2014.03.018>.
- Arrigo, K. R. and G. L. van Dijken (2015), Continued increases in Arctic Ocean primary production, *Prog. Oceanogr.*, *136*, 60-70, <http://dx.doi.org/10.1016/j.pocean.2015.05.002>.
- Belanger, S., M. Babin, and J.-E. Tremblay (2013), Increasing cloudiness in Arctic damps the increase in phytoplankton primary production due to sea ice receding, *Biogeosciences*, *10*, 4087–4101.
- Brown, Z. W., K. Lowry, M. A. Palmer, and G. L. van Dijken, M. M. Mills, R. S. Pickart and K. R. Arrigo (2015a), Characterizing the subsurface chlorophyll a maximum in the Chukchi Sea and Canada Basin, *Deep-Sea Res. Part II*, *118*, 88–104.

- Brown, Z. W., K.L. Casciotti, R.S. Pickart, J.H. Swift and K. R. Arrigo, K.R. (2015b), Aspects of the marine nitrogen cycle of the Chukchi Sea shelf and Canada Basin. *Deep-Sea Res. Part II*, 118, 73-87.
- Carmack, E.C. (2000), The Arctic Ocean's freshwater budget: sources, storage and export. In: Lewis, E.L., Jones, E.P., Lemke, P., Prowse, T.D., Wadhams, P. (Eds.), *The Freshwater Budget of the Arctic Ocean*. Kluwer Academic Publishers, The Netherlands, pp. 91–126.
- Cavalieri, D. J., C. L. Parkinson, P. Gloersen, and H. J. Zwally (1996), Sea Ice Concentrations from Nimbus-7 SMMR and DMSP SSM/I-SSMIS Passive Microwave Data, Version 1. Boulder, Colorado USA, NASA National Snow and Ice Data Center Distributed Active Archive Center, doi: <http://dx.doi.org/10.5067/8GQ8LZQVL0VL>.
- Chang, B. X. and A. H. Devol (2009), Seasonal and spatial patterns of sedimentary denitrification rates in the Chukchi Sea, *Deep-Sea Res., Part II*, 56, 1339–1350.
- Coachman, L.K, Aagaard, K. and R.B. Tripp (1975), Bering Strait, the regional physical oceanography, University of Washington Press, Seattle, 172 pp.
- Codispoti, L. A., C. N. Flagg, V. Kelly, and J. H. Swift (2005), Hydrographic conditions during the 2002 SBI process experiments, *Deep-Sea Res., Part II*, 52, 3199-3226.
- Codispoti, L. A., C. N. Flagg, and J. H. Swift (2009), Hydrographic conditions during the 2004 SBI process experiments, *Deep-Sea Research, Part II*, 56(17), 1144-1163.
- Codispoti, L. A., V. Kelly, A. Thessen, P. Matrai, S. Suttles, V. Hill, M. Steele, and B. Light (2013), Synthesis of primary production in the Arctic Ocean: III. Nitrate and phosphate based estimates of net community production, *Prog. Oceanogr.* 110, 126-150.
- Cota, G. F., L. R. Pomeroy, W. G. Harrison, E. P. Jones, F. Peters, W. M. Sheldon, and T. R. Weingartner (1996), Nutrients, primary production and microbial heterotrophy in the southeastern Chukchi Sea: Arctic summer nutrient depletion and heterotrophy, *Mar. Ecol. Prog. Ser.*, 135(1-3), 247-258.

- Devol, A. H., L. A. Codispoti, and J. P. Christensen (1997), Summer and winter denitrification rates in western Arctic shelf sediments, *Cont. Shelf Res.*, *17*, 1029–1033, doi:10.1016/S0278-4343(97)00003-4.
- Eppley, R. W., and B. J. Peterson (1979), Particulate organic-matter flux and planktonic new production in the deep ocean, *Nature*, *282*(5740), 677-680.
- Granger, J., M. G. Prokopenko, D. M. Sigman, C. W. Mordy, Z. M. Morse, L. V. Morales, R. N. Sambrotto, and B. Plessen (2011), Coupled nitrification–denitrification in sediment of the eastern Bering Sea shelf leads to ¹⁵N enrichment of fixed N in shelf waters, *J. Geophys. Res.*, *116*, C11006, doi:10.1029/2010JC006751.
- Haines, J. R., R. M. Atlas, R. P. Griffiths, and R. Y. Morita (1981), Denitrification and nitrogen fixation in Alaskan continental–shelf sediments, *Appl. Environ. Microbiol.*, *41*, 412–421.
- Hansell, D. A., T. E. Whitledge, and J. J. Goering (1993), Patterns of nitrate utilization and new production over the Bering–Chukchi shelf, *Cont. Shelf Res.*, *13*, 601-527.
- Hartnett, H. (1998), *Organic Carbon Input, Degradation and Preservation in Continental Margin Sediments: An Assessment of the Role of a Strong Oxygen Deficient Zone*, Univ. of Wash., Seattle.
- Henriksen, K., T. H. Blackburn, B. A. Lomstein, and C. P. McRoy (1993), Rates of nitrification, distribution of nitrifying bacteria and inorganic N fluxes in northern Bering Chuckchi shelf sediments, *Cont. Shelf Res.*, *13*, 629–651, doi:10.1016/0278-4343(93)90097-H.
- Hessen, D. O., H. Frigstad, P. J. Faerovig, M. W. Wojewodzic, and E. Leu (2012), UV radiation and its effects on P-uptake in arctic diatoms, *J. Exp. Mar. Biol. Ecol.*, *411*, 45-51.
- Hill, V. and G. Cota (2005), Spatial patterns of primary production on the shelf, slope and basin of the Western Arctic in 2002, *Deep-Sea Res., Part II*, *52*, 3344–3354.
- Holm-Hansen, O., C. J. Lorenzen, R. W. Holmes, and J. D. H. Strickland (1965), Fluorometric determination of chlorophyll, *ICES J. Mar. Sci.*, *30*(1), 3–15, doi:10.1093/icesjms/30.1.3.
- Koike, I., and A. Hattori (1979), Estimates of denitrification in sediments of the Bering Sea shelf, *J. Geophys. Res.*, *26*, 409–415.

- Lowry, K. E., R.S. Pickart, M.M. Mills, Z.W. Brown, G.L. van Dijken, N.R. Bates and K. R. Arrigo (2015), The influence of winter water on phytoplankton blooms in the Chukchi Sea. *Deep-Sea Res. Part II*, 118, 53-72.
- Martin, J., J-É Tremblay, J. Gagnon, G. Tremblay, A. Lapoussière, C. Jose, M. Poulin, M. Gosselin, Y. Gratton, and C. Michel (2010), Prevalence, structure and properties of subsurface chlorophyll maxima in Canadian Arctic waters, *Mar. Ecol. Prog. Ser.*, 412, 69-84, doi: 10.3354/meps08666.
- Padman, L., and S. Erofeeva (2004), A barotropic inverse tidal model for the Arctic Ocean, *Geophys. Res. Lett.*, 31(2), doi:10.1029/2003GL019003.
- Pickart, R. S., G. W. K. Moore, C. Mao, F. Bahr, C. Nobre, and T. J. Weingartner (2016), Circulation of winter water on the Chukchi shelf in early Summer, *Deep-Sea Res. Part II*, 130(C), 56–75, doi:10.1016/j.dsr2.2016.05.001.
- Spall, M.A. (2007), Circulation and water mass transformation in a model of the Chukchi Sea, *J. Geophys. Res.*, 112, C05025, doi:05010.01029/02005JC002264.
- Varela, D. E., D. W. Crawford, I. A. Wrohan, S. N. Wyatt, and E. C. Carmack (2013), Pelagic primary productivity and upper ocean nutrient dynamics across Subarctic and Arctic Seas, *J. Geophys. Res. Oceans*, 118, 7132–7152, doi:10.1002/2013JC009211.
- Wang, J., G. F. Cota, and J. C. Comiso (2005), Phytoplankton in the Beaufort and Chukchi seas: distribution, dynamics, and environmental forcing, *Deep-Sea Res., Part II*, 52(24-26).
- Weingartner, T. J., K. Aagaard, R. Woodgate, S. Danielson, Y. Sasaki, and D. J. Cavalieri (2005), Circulation on the north central Chukchi Sea shelf, *Deep-Sea Res. Part II*, 52, 3150 - 3174.
- Weingartner, T.J., E. Dobbins, S. Danielson, P. Winsor, R. Potter, and H. Statscewich (2013), Hydrographic variability over the northeastern Chukchi Sea shelf in summer-fall 2008-2010, *Cont. Shelf Res.*, 67, 5-22.

Woodgate, R.A., K. Aagaard, T.J. Weingartner (2005), A year in the physical oceanography of the Chukchi Sea: Moored measurements from autumn 1990-1991. *Deep-Sea Res., Part II*, 52, 3116-3149.

Zhang, J., Y. H. Spitz, M. Steele, C. Ashjian, R. Campbell, L. Berline and P. Matrai (2010), Modeling the impact of declining sea ice on the Arctic marine planktonic ecosystem, *J. Geophys. Res.*, 115, C10015.

Zhang, J., C. J. Ashjian, R. Campbell, and Y. H. Spitz (2015), The influence of sea ice and snow cover and nutrient availability on the formation of massive under-ice phytoplankton blooms in the Chukchi Sea, *Deep-Sea Res. Part II*, 118, 122–135, doi:10.1016/j.dsr2.2015.02.008.

Figure Legends

Figure 1. Map of the SUBICE study region showing the stations used in the study (black squares) overlaid on the concentration of chlorophyll *a* in open water and sea ice (calculated from the sea ice algorithm of *Cavaliere et al.* [1996]) on 15 June 2014. A schematic representation of the main flow paths of Pacific-origin water on the Chukchi shelf (grey lines) are included. The solid purple line denotes the 1000 m isobath.

Figure 2. Potential temperature versus salinity diagram for stations shown in Fig. 1. Colors denote nitrate concentration. MW = meltwater, NVWW = Newly ventilated winter water, RWW = Remnant winter water.

Figure 3. 3-D sections of (A) potential temperature, (B) salinity, and (C) nitrate concentration for a subset of the SUBICE station grid. Gray lines indicate flow paths inferred using the ADCP data. Only stations sampled early in the season prior to appreciable phytoplankton growth have been included. Graphics created using Ocean Data View and Ocean3D.

Figure 4. Relationship between nitrate concentration and salinity for stations shown in Fig. 3. Colors denote the day of year that the samples were collected. Dark black line is the linear fit of the data ($y = 5.631x - 169.47$, $R=0.84$, $p < 0.001$). Light black lines are the regressions of nitrate versus salinity for three different years (and all three years combined) from the southeastern Bering Sea [*Hansell et al.*, 1993], illustrating generally higher nitrate concentrations than observed during our study.

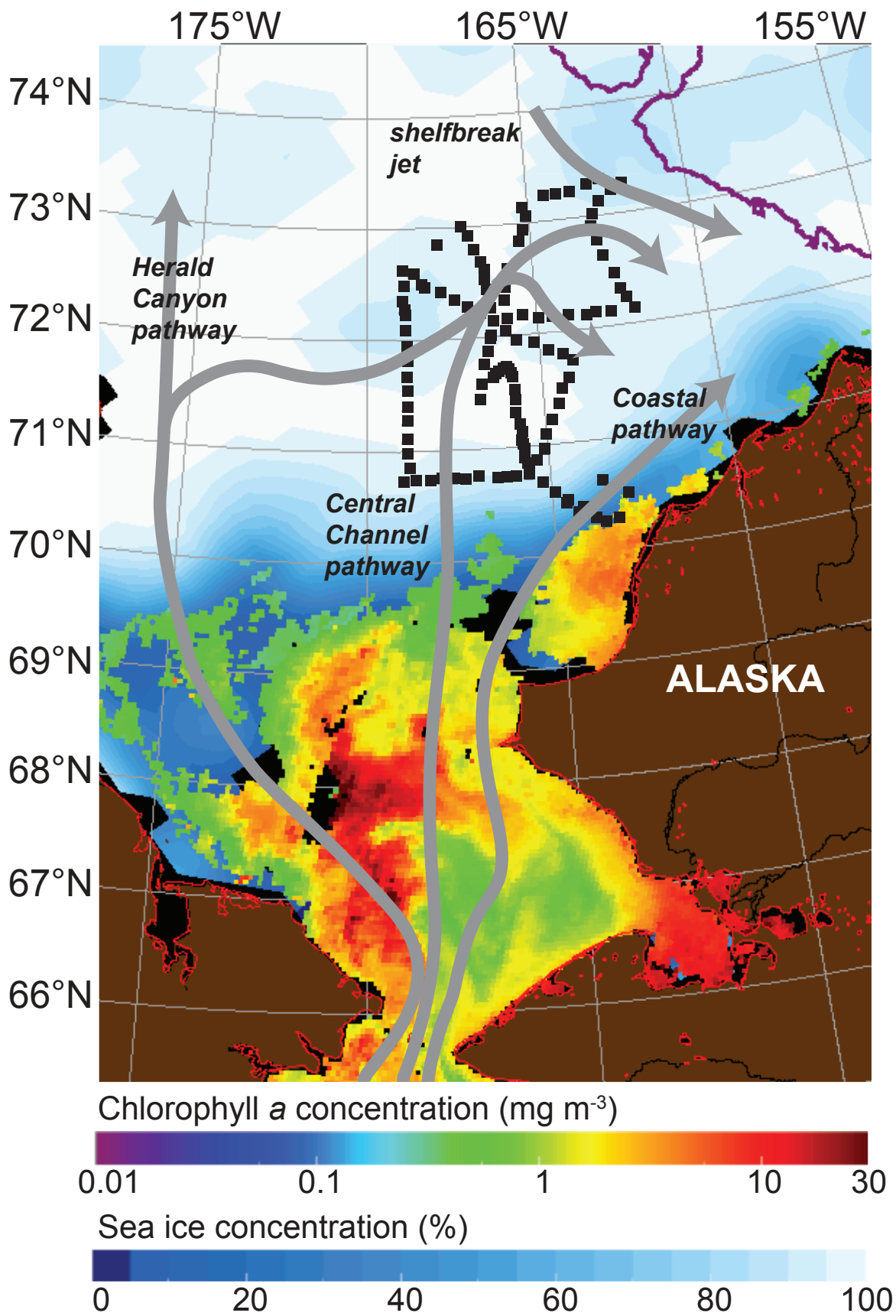


Figure 1. Map of the SUBICE study region showing the stations used in the study (black squares) overlaid on the concentration of chlorophyll *a* in open water and sea ice (calculated from the sea ice algorithm of Cavalieri et al. [1996]) on 15 June 2014. A schematic representation of the main flow paths of Pacific-origin water on the Chukchi shelf (grey lines) are included. The solid purple line denotes the 1000 m isobath.

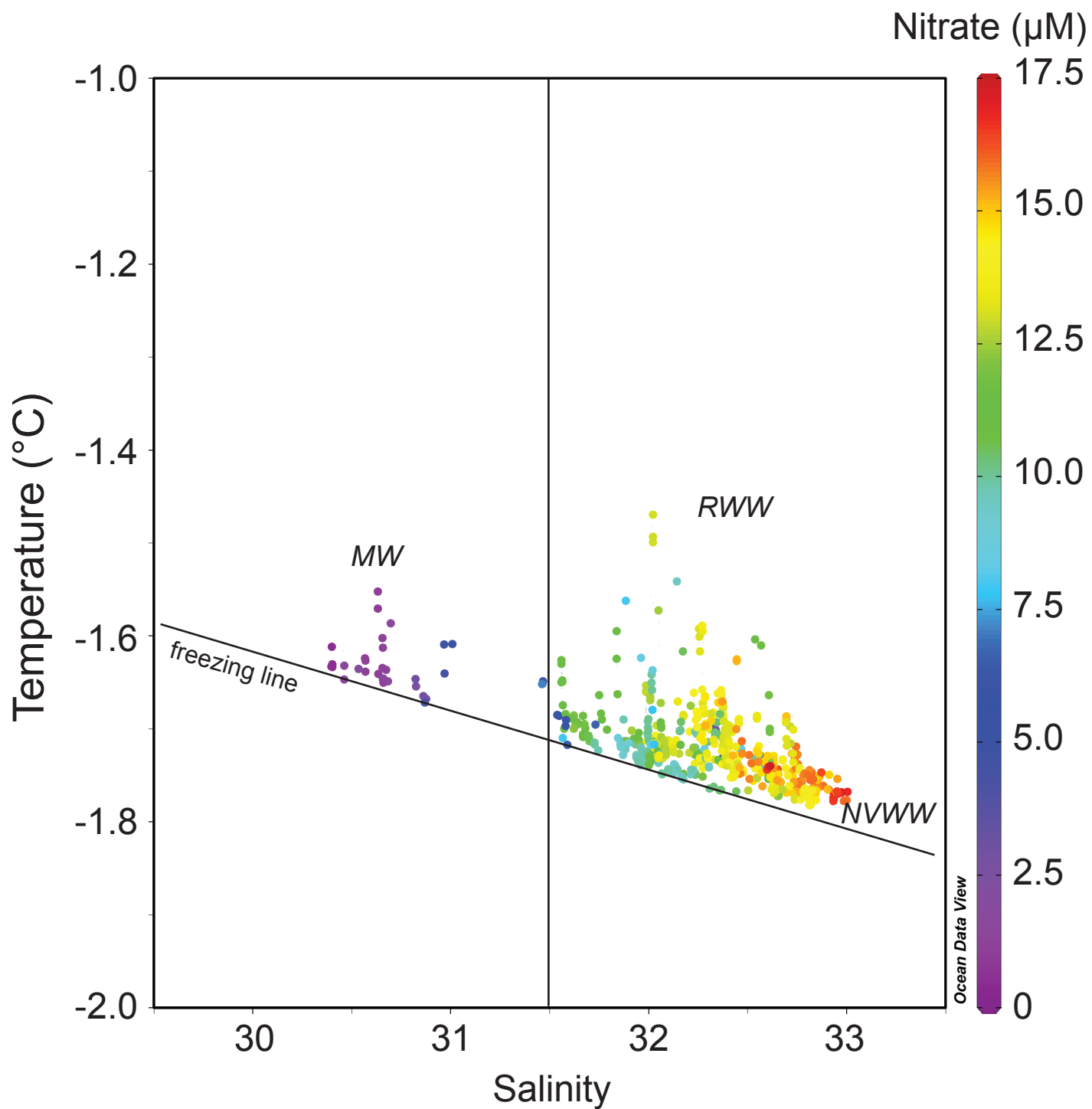


Figure 2. T-S diagram for stations shown in Fig. 1. Colors denote nitrate concentration. MW = meltwater, NVWW = Newly ventilated winter water, RWW = Remnant winter water.

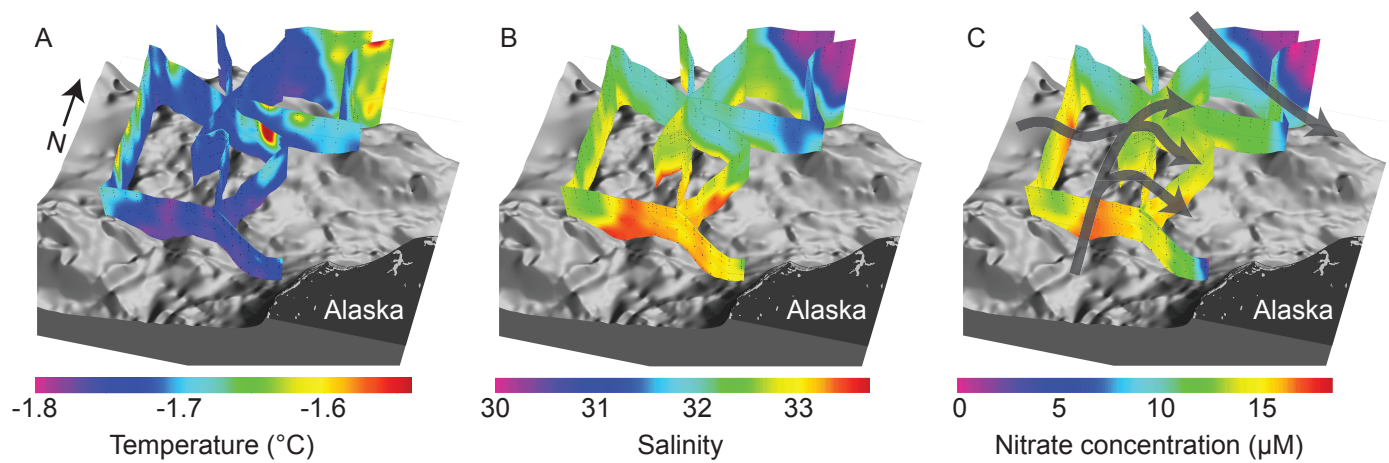


Figure 3. 3-D sections of (A) temperature, (B) salinity, and (C) nitrate concentration for a subset of the SUBICE station grid. Gray lines indicate inferred flow paths. Only stations sampled early in the season prior to appreciable phytoplankton growth have been included. Graphics created using Ocean Data View and Ocean3D.

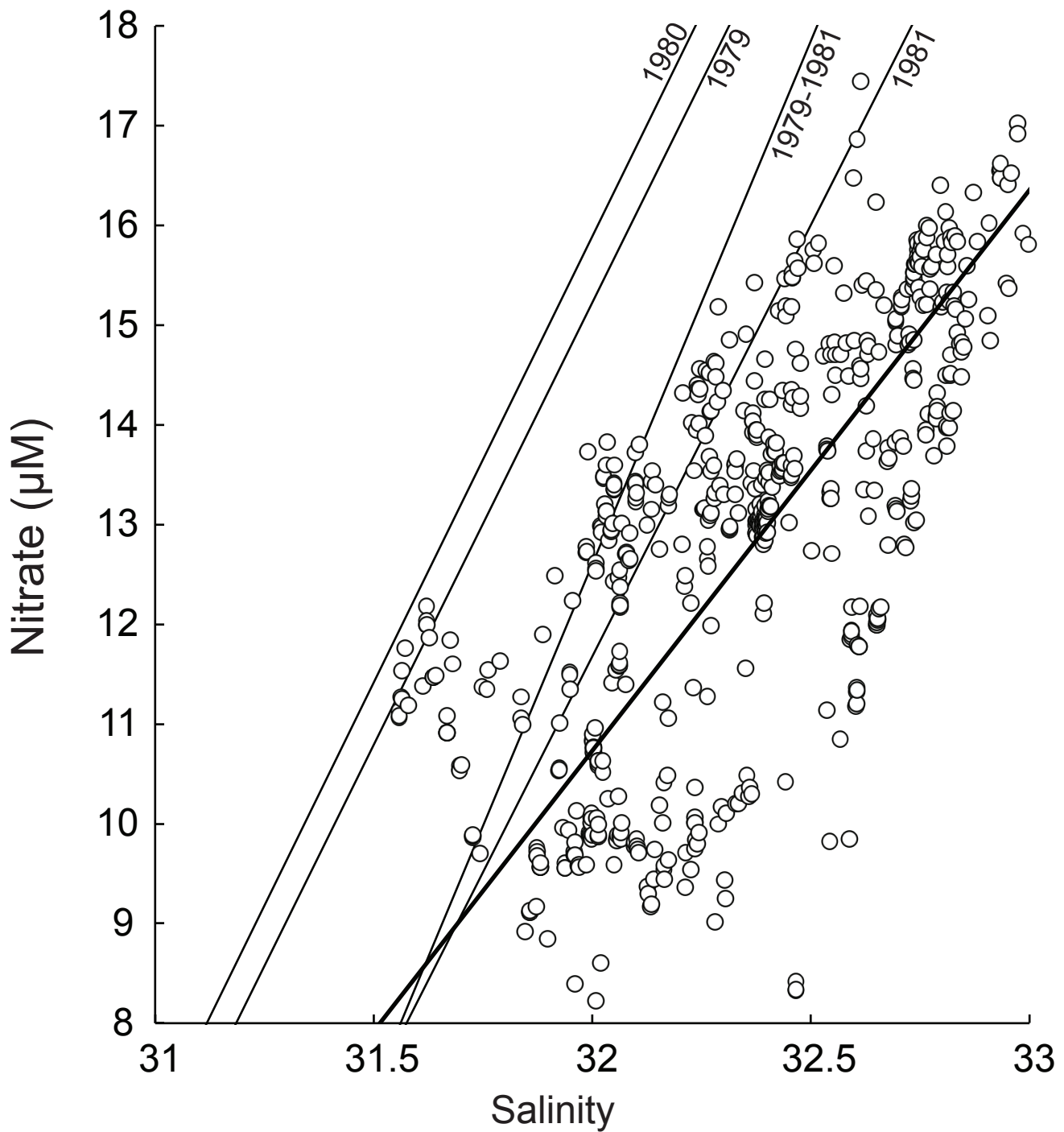


Figure 4. Relationship between nitrate concentration and salinity for stations shown in Fig. 3. Colors denote the day of year that the samples were collected. Dark black line is the linear fit of the data ($y = 5.631x - 169.47$, $R=0.84$, $p < 0.001$). Light black lines are the regressions of nitrate versus salinity for three different years (and all three years combined) from the southeastern Bering Sea [Hansell *et al.*, 1993], illustrating generally higher nitrate concentrations than observed during our study.